



City Research Online

City, University of London Institutional Repository

Citation: Fu, F. (2013). Dynamic response and robustness of tall buildings under blast loading. *Journal of Constructional Steel Research*, 80, pp. 299-307. doi: 10.1016/j.jcsr.2012.10.001

This is the accepted version of the paper.

This version of the publication may differ from the final published version.

Permanent repository link: <http://openaccess.city.ac.uk/20083/>

Link to published version: <http://dx.doi.org/10.1016/j.jcsr.2012.10.001>

Copyright and reuse: City Research Online aims to make research outputs of City, University of London available to a wider audience. Copyright and Moral Rights remain with the author(s) and/or copyright holders. URLs from City Research Online may be freely distributed and linked to.

City Research Online:

<http://openaccess.city.ac.uk/>

publications@city.ac.uk

Dynamic Response and Robustness of Tall Buildings under Blast Loading

Feng Fu*

School of Engineering, Design and Technology, University of Bradford, BD7 1DP

Abstract

Recently, extensive research has been focused on the progressive collapse analysis of the multi-storey buildings. However, most of the research is based on the Alternative Path Method (APM) with sudden removal of the columns, ignoring the duration of the blast load working on the structures. In this paper, a 3-D numerical model with the direct simulation of blast load is proposed to study the real behaviour of a 20 storey tall building under the blast loading. A typical package bomb charge of 15 kg was detonated on the 12th floor. The corresponding dynamic response of structure was studied in details. The robustness of the building under blast load was assessed. Comparison between the proposed method and the APM was also made. It is found that, due to the uplift and downward pressure working on the slab, the column force under the direct blast simulation method is smaller than that of the alternative path method. The method to enhance the robustness of the buildings is also recommended.

Keywords: progressive collapse, blast, arrival time, duration, overpressure

1 INTRODUCTION

Recently, the special design requirement of buildings against blast load becomes more and more important for the safety of the occupants. Explosions can be categorized on the basis of their nature. It can be a bomb, a gas-chemical explosion or an airplane attack etc. An explosion can cause damage on the building's structural frames, which may cause structural collapse. The airplane attack on 911 brought great attention to the researchers on the response of multi-storey buildings due to extreme loading conditions such as blast. More and more researchers started to refocus on the causes of progressive collapse in building structures, seeking rational methods for the assessment and enhancement of structural robustness under extreme accidental events. In the United States, the Department of Defense (DoD) [1] and the General Services Administration (GSA) [2] provide detailed information and guidelines regarding methodologies to resist progressive collapse of building structures. Both employ the

* Corresponding author
E-mail address: cenffu@yahoo.co.uk

alternate path method (APM). The methodology is generally applied in the context of a 'missing column' scenario to assess the potential of progressive collapse by directly removing a column. However, in this method, the damage to the adjacent structural members that might be induced by blast loads is neglected. These simplifications may lead to inaccurate predictions of the structural collapse.

Other efforts have also been made during the past decades to develop the methods of structural analysis and design guidance to resist blast loads. The UK SCI publication 244 [3] provides a guidance on the design of commercial and public buildings where there is a requirement to provide protection against the effects of explosions caused by the detonation of explosives. A philosophy for the design of buildings to reduce the effects of attack is introduced and a design procedure is proposed. The robustness of buildings and the prevention of disproportionate collapse are also discussed. In United States, FEMA 426 [4] provides the design measurements to reduce physical damage to the structural and non-structural components of building and related infrastructures during conventional bomb attacks, as well as attacks using chemical, biological and CBR agents. Kambouchev et al [5] discussed the nonlinear compressibility effects in fluid-structure interaction and their implications on the air-blast loading of structures. Blanc et al [6] discussed empirical method to estimate the blast loading. Beshara [7] discussed the modeling of blast loading on aboveground structures. Remennikov et al [8] provided an accurate prediction of the effects of adjacent structures on the blast loads on a building in urban terrain. Luccioni [9] performed the tests to assess the concrete pavement slab under blast loads.

However, due to the huge cost, it is almost impossible to investigate the response of the multi-story buildings against blast loads with full-scale experimental tests. Therefore, advanced numerical tools such as the finite element method become the main approach for the related research. The analysis and design of structures subjected to blast loads require a detailed understanding of blast phenomena and the dynamic response of various structural elements. Some numerical modeling has been done in the past decades. Børvik et al [10] investigated if a pure Lagrangian formulation could be applied to determine the structural response in a specified blast load problem. Luccioni et.al [11] performed a detailed analysis of the structural failure of a reinforced concrete building caused by a blast load. However, most of the current numerical modeling research is involved with massive computational time and the model is difficult to build due to its complexity. Therefore, for designers, it is imperative to establish a simple modeling method to study the detailed behavior of the building after the blast denotation.

To solve this problem, in this paper, using modeling techniques developed by Fu [12] with ABAQUS [13], a 3-D finite element model representing a 20-storey building was built to perform the blast analysis. A simplified direct simulation method of blast load is applied here. The proposed method can apply the blast loads directly on the frames and the floors of the building. The nonlinear material behaviour and dynamic effects

are also included in the simulation. The proposed method requires substantially less computational effort as compared to other direct numerical simulations. Based on this model, detailed response and possible collapse mechanism of the multi-storey buildings are also discussed. The measures to increase the robustness of the high-rise building in the future design are also recommended. To check the effectiveness of the Alternative path method, an identical model was also built to investigate the behaviour of the buildings with the ‘sudden column removal’ approach. Comparison between these two methods was also made.

2 3D FINITE ELEMENT MODEL

As shown in Fig 1, a three-dimensional finite element model was created by Fu [12] using the ABAQUS [13] package. This model simulates the full structural framing of a typical high-rise building in the current construction practice with full composite action of the composite slab. It replicates a 20-Storey steel composite building with the grid spacing of 7.5m in both directions. The main lateral stability of the building is provided by cross bracings (as shown in Fig.1) in the exterior frame at the four facades. The steel beam to column connections and the bracing to column connections are simulated as fully pinned. The continuity across the connection is maintained by the composite slab acting across the top of the connection. The floor height is 3 m for each floor. The slab thickness is 130mm. All the structural steel members are using grade S355 steel. The columns are British universal column UC356X406X634 for ground floor to level 6, UC356X406X467 for level 7 to level 13, UC356X406X287 for level 14 to level 19, all the beams are British universal beam UB533X210X92. The cross bracings are British circular Hollow section CHCF 273X12.5. The section properties are shown in Table1. The section sizes of the structural steel members were determined followed the capacity design principles of British standards [14],[15].

2.1 Modelling techniques

All the beams and columns were simulated using *BEAM elements. The orientation of a beam cross-section is defined in ABAQUS in terms of a local, right-handed (t , n_1 , n_2) axis system, where t is the tangent to the axis of the element, positive in the direction from the first to the second node of the element. n_1 and n_2 are basis vectors that define the local 1- and 2-directions of the cross-section. n_1 is referred to as the first beam section axis, and n_2 is referred to as the normal to the beam(see Fig.2).

The slabs were simulated using the four node *Shell elements. Reinforcements were represented as a smeared layer in each shell element using the *REBAR elements and were defined in both slab directions. In ABAQUS [13], the local material 1- and 2-directions lie in the plane of the shell. The default local 1-direction is the projection of the global 1-axis onto the shell surface. If the global 1-axis is normal to the shell surface, the local 1-direction is the projection of the global 3-axis onto the shell surface. The local 2-direction is perpendicular to the local 1-direction in the surface of the shell, so that the local 1-direction, local 2-direction, and the positive normal to the

surface form a right-handed set (see Fig. 3).

The beam and shell elements were then coupled together using rigid beam constraint equations to give the composite action between the beam elements and the concrete slabs. The concrete was modeled using a concrete damage plasticity model. The material properties of all the structural steel components and slab reinforcement were modeled using an elastic-plastic material model incorporating the material nonlinearity. The model is supported at the bottom as shown in Fig.1. The mesh representing the model was studied and is sufficiently fine in the areas of interest to ensure that the developed forces can be accurately determined. The model was validated against the test result of [16], good agreement was obtained. The detailed description of the modeling technique is shown in Fu [12].

2.2 Material behaviour of structural members at high strain rate

The nonlinear behaviour and dynamic effects of the material due to blast or impact loading are also considered in the simulation.

The mechanical properties of the structural steel members under blast loading are affected noticeably by the rate at which straining takes place. In the proposed model, the dynamic design yield stress of the steel $F_{y,des}$ for bending is determined by[3]:

$$F_{y,des} = a \text{ (DIF) } F_y \quad (1)$$

Where,

a is a factor that takes into account the fact that the yield stress of a structural component is generally higher than the minimum specified value given in BS 5950[15]. Following guidance [3], for S275 and S355 steels, $a = 1.10$.

DIF is the Dynamic increase factors for structural steels can be checked in Table 9.1 of [3]

In the proposed model, the dynamic increase factor for the reinforced concrete elements used in composite design is calculated follows the Table 9.3 of [3].

3 APPLICATION OF BLAST LOAD DATA

As it is discussed in [6], to precisely evaluate the shock propagation around the structure and the structure's response, using a fluid-structure interaction method is possible. However, it will generate big models. Another possibility is to use the empirical model to compute the load on the structure. This solution is computational effective and is used in this paper with the program ATBLAST [17]. It will be explained in details in this section.

3.1 Blast attack scenarios

There are many ways in which an explosive device may deliver an attack. As it is stated in [3], there are several conventional devices like Vehicle bombs, Package bombs, Mortar bombs, Culvert bombs and Incendiary devices. In this paper, the scenario of Package bombs is selected for the study, as this type of attack is more difficult to be prevented than other attack scenarios such as vehicle bombs.

3.2 Determination of the blast-wave

The principle of the scaling law is used extensively to determine blast-wave characteristics in most design guidance such as TM5-1300 [18]. It is based on the conservation of momentum and geometric similarity. The empirical relationship, formulated independently by Hopkinson [19] and Cranz [20], is described as cube-root scaling law and is defined as:

$$Z = \frac{R}{W^{1/3}} \quad (2)$$

Where,

Z is the scaled distance, with units (m/kg^{-1/3})

R is the range from the centre of the charge

W is the mass of spherical TNT charge (kg).

In this paper, a general purpose program ATBLAST [17] is used here for predicting explosive effects, which is commercial software of evaluating potential blast damage. It is designed based on the empirical formula of TM5-1300 [18]. It calculates the blast loading parameters from an open hemispherical explosion based on the distance from the device. The program allows the user to enter the weight of explosive charge, a reflection angle, minimum and maximum ranges to the charges and the calculation interval. From this information, it can calculate the shock velocity, time of Arrival, overpressure, impulse and load duration of the blast loading.

As it is stated in [3] that, it is usually adequate to assume that the decay (and growth) of blast overpressure is linear. For the positive overpressure phase, a simplification is made where the impulse of the positive phase of the blast is preserved and the decay of overpressure is assumed to be linear as it is shown in Fig.4. This simplification is also applied in ATBLAST [17]. The purpose of the paper is to provide a fast blast evaluation, and to investigate the response of the building when the blast wave just starts to act on the structure. Therefore, to simplify the model, the effect of blast wave reflections on structural and non-structural elements after the denotation was neglected.

In this paper, a subroutine program with Visual BASIC language is designed by the author, which can transfer the blast load profile worked out by ATBLAST [17] to the

20-storey prototype model built in ABAQUS. In the simulation, the blast load was applied as an area load working directly on the slabs and line load directly on the beams and columns with all the related information as shown in Fig.5. For the applied blast loading, the time of arrival and load duration are all different due to their distance to the blast charge locations. Therefore, the propagation of the blast wave was also simulated. This is shown in Fig.6, which clearly shows the blast pressure propagation through the slab at different time. Therefore, the response of the 20 storey prototype building can be evaluated.

3.3 Numerical analysis

Using general purpose program ABAQUS, the response of the prototype building under the blast load is assessed here using nonlinear dynamic analysis method with 3-D finite element technique. The loads are computed as dead loads (which is the self-weight of the floor) plus 25% of the live load in accordance with the acceptance criteria outlined in GSA guidelines [2].

The static analysis with the dead and live load loaded to the building was conducted in the first second as a static step. After this step, a blast load of 15 kg TNT detonated at location of column A1 on level 12 as it is shown in Fig1.a. This is to simulate the typical charge weight for a package bombs indicted in SCI 244 [3] table 6.1 occurs inside an office building. Fig 6 is the Pressure of distributed blast load on element surface at different selected time. It clearly shows the blast wave pressure propagating from the charging location to the adjacent structural members on level 12.

The simulations were conducted with 5% mass damping. In the analysis, the internal forces, such as axial force, shear force, bending moment, displacements and rotations for each of the members involved in the scenario are recorded.

4 RESPONSE OF THE BUILDING UNDER BLAST LOAD

To facilitate the following discussion, the columns and beams are designated as follows according to the grid line shown in Fig1.b. For instance, Column C1 stands for the column at the junction of grid C and grid 1. Beam E1-D1 stand for the beam on grid 1 starting from grid E to grid D.

In order to compare the result with the Alternative path method, another identical model was also built. This model used the APM for the analysis. In the analysis, the column A1 on level 12 was suddenly removed at the same location of its counterpart. The response of the building was recorded, and the comparison of the two methods is shown in Table2.

The response of the structure was extracted from the 3-D finite element model. And the results are shown in the following sections.

4.1 Behaviour of the beams

Fig.7 to Fig.9 shows the response of the beam B1-A1 at level 13, one floor above the blast charge location. From Fig.7, it can be seen that, from Time=0 to Time=1 second, the static step was taking place, the axial force increased linearly, it is shown as a slope line in the Figures. At second 1, the blast was detonated, the axial force, shear force and bending moment of the beam started to increase. At time 1.03S, the axial force reached a peak value of 884kN, which is due to the arrival of the peak of blast wave. This force then started to oscillate until it is finally settled. The similar response can be found for bending moment as well. Fig. 8 is the plastic stain of beam B1-A1 at level 13, it can be seen that, after the denotation of the blast, the plastic strain is increased from 0 to 0.008, which indicates the onset of yielding in beam B1-A1.

According to the principle of the scaling law, the blast load reduces quickly when the distance increases. This can be observed in Fig.10 to Fig.11. They show the response of the beam D1-C1 at level 13, which locates two bays away to the blast charge location. It can be seen that, compared with beam B1-A1, the response of beam D1-C1 decreased dramatically. Fig.12 is the plastic strain observed in beam D1-C1, no plastic strain is observed, which indicates that the beam is still in the elastic stage.

4.2 Behaviour of the columns

4.2.1 Shear force comparisons of columns at different location

The car bomb attack happened in Oklahoma City in 1995 shows that, except the failure of the column where the bomb was detonated, the adjacent columns were also sheared off. Fig 13 is the shear force response of the column B1 on level 12 which is adjacent to the blast charge location. It can be seen that at time 1.01S, the shear force of the column reach a peak value 220 kN. As this shear force is quite large, so it could not be ignored. Therefore, one way to mitigate the collapse of the building is to enhance the shear capacity of the column.

The shear forces of columns at other locations are chosen for the study as well, as it is shown in Fig 14 to Fig.15. It can be seen that, with the increasing of the distance, the response of the column decreased dramatically, the effect of the blast loading become quite small, can be ignored.

4.2.2 Axial force comparisons of columns at different location

In order to investigate the axial force of the columns, the columns at different location are chosen for the studies. Fig 16 is the axial force response of the column B1 on level 12. It can be seen that at time 1.006s, the compressive force of the column reached a peak value -1460kN, after that the force started to decrease until it become in tension.

Table 2 is the comparison between the blast load direct simulation method and APM, It can be seen from that, with the Alternative Path Method, after the column was suddenly removed, the compressive forces of the adjacent columns increased due to

the redistribution of the load. However, in real scenario of blast denotation, as the pressure wave continues to expand into the building, upward pressures are applied to the ceilings and downward pressures are applied to the floors, which makes the column in tension. Therefore, it reduced the compression load in the columns. Therefore, the alternative path method is more conservative in predicting the axial force in the adjacent columns.

The axial force of the columns at different location is shown in Fig. 17 to Fig.18. Where, Fig. 18 is the response of the column D4 at level 12. Following the principle of the scaling law, It can be seen that, compared with column A1 at level 12, the axial forces of D4 was almost kept unchanged after the blast charge.

4.2.3 Bending moment comparisons of columns at different location

Fig.19 and Fig.20 are the response of the bending moment of columns at different location on level 12. It can be seen that the large moment is observed in column B1. The bending moment reduced quickly when the distance from the location of the column to the blast charge location increased.

4.2.4 Plastic strain comparisons of columns at different location

Fig. 21 and Fig.22 are the response of plastic stain of columns at different location on level 12. It can be seen that, after the denotation of the blast, the plastic strain of column A1 and B1 were observed, which indicates the onset of yielding in column B1 and A1. When the yielding develops into certain stage, the plastic hinge will start to form. Therefore, another possible way to mitigating the collapse is to increase the ductility of the steel frame.

However, as it is shown in Fig.23 that, for column B2, which locates farer to the blast charge location than column B1, no plastic strain was observed. A further check of the plastic strain of column C1 was also made, no plastic strain was observed as well. This indicted that the yielding of the column only limited to a small area inside the building.

4.3 Behavior of the slabs

Fig. 24 shows tensor of the plastic strain in the composite slab of the whole building which also shows the crack pattern of the slab. It can be seen that, most cracks are concentrated near the blast charge location on floor 12 and 13. No cracks are observed in other areas. Fig.25 is the plastic strain in slab A1-B1-B2-A2 on level 13, which indicate the crack development in this slab.

4.4 Collapse potential of the building

It is well known that the columns play an important role in the prevention of the collapse of the building. Following Progressive collapse analysis and design guidelines [2], the collapse potential of the building is checked here starting from the columns. From numerical analysis in section 4.2.4, it can be seen that, the three

columns A1, B1 and A2 (due to symmetry, the force in B1 and A2 are identical) at level 12 near the blast charge location started to yield. However, a manual checking in accordance to BS5990 [15] is made, it shows that the maximum axial force, bending moment and shear force obtained from the analysis does not exceed the capacity of the columns, the three columns did not fail, nor did the adjacent columns. Therefore, no collapse of the whole building was triggered.

4.5 Discussion of Analysis

The above analysis shows that, the blast load decreases dramatically with the increasing of the distance, beyond certain distance, the effect of blast pressure can be ignored. It can also be seen that, the structural steel member yielding and the slab crack are mainly concentrated near the blast charge location. The effect to the remaining structure is quite small. Therefore, for the building designed using the current design guidance, the small scale blast such as the package bomb can only cause localized structural member damage, it is hard to trigger the collapse of the whole building, as long as the alternative path can be provided for the load to be redistributed to the adjacent structural members. It can also be suggested that, one way to prevent the progressive collapse of the building under blast load is to enhanced shear capacity and increase the ductility of the column.

5 CONCLUSIONS

In this paper, the numerical simulation of a tall building under a 15 Kg package bomb is conducted. The dynamic behaviour of the building is studied in details. The robustness of the tall building under the blast load is studied. The main conclusions are made as follows:

1. Due to the uplift and downward pressures working on the slabs, the column force under the direct blast simulation method is smaller than that of the alternative path method, so the conventional alternative path method is more conservative in assessing the robustness of the building.
2. The Alternative Path Method ignores the huge shear force applied to the column due to the blast loading. Therefore, when using the APM method to evaluate the robustness of the building, the shear capacity of the column should also be checked.
3. To prevent the progressive collapse of the building under blast load, the shear capacity and the ductility of the column need to be enhanced.
4. For the buildings designed using the current design guidance, the small scale blast such as the package bomb will normally cause localized structural member damage, and it hardly triggers the collapse of the whole building, as long as the alternative path can be provided for the load to be redistributed.

REFERENCE

- [1] Unified Facilities Criteria (UFC)-DoD. Design of Buildings to Resist Progressive Collapse, Department of Defense, 2005.
- [2] GSA. Progressive collapse analysis and design guidelines for new federal office buildings and major modernization projects. The U.S. General Services Administration; 2003.
- [3] E YANDZIO, M GOUGH, Protection of Buildings against Explosions. SCI PUBLICATION 244, (1999)
- [4] Risk Management series, reference manual to mitigate potential terrorist Attacks against buildings, FEMA426, Dec 2003
- [5] N. Kambouchev, L. Noels, and R. Radovitzky, Nonlinear compressibility effects in fluid-structure interaction and their implications on the air-blast loading of structures, *J. Appl. Phys.* 100, 063519 (2006)
- [6] G. Le Blanc, M.Adoum, V.Lapoujade, External blast load on structures – Empirical approach, 5 th European LS-DYNA Users conference.
- [7] F.B.A. Beshara, Modelling of blast loading on aboveground structures—I. General phenomenology and external blast, *Computers & Structures* Volume 51, Issue 5, 3 June 1994, Pages 585–596
- [8] Alex M. Remennikov, Timothy A. Rose, Modelling blast loads on buildings in complex city geometries *Computers & Structures*, Volume 83, Issue 27, October 2005, Pages 2197-2205
- [9] B. M., Luccioni, Mariela Luege, Concrete pavement slab under blast loads *International, Journal of Impact Engineering* 32, (2006) 1248–1266
- [10] T. Børvik, A.G. Hanssen, M. Langseth and L. Olovsson, Response of structures to planar blast loads – A finite element engineering approach, *Computers & Structures*, Volume 87, Issues 9-10, May 2009, Pages 507-520
- [11] B. M. Luccioni, R. D. Ambrosini, R. F. Danesi, Analysis of building collapse under blast loads, *Engineering Structures*, Volume 26, Issue 1, January 2004, Pages 63-71
- [12] Feng Fu, Progressive collapse analysis of high-rise building with 3-D finite

element modelling method, Journal of Constructional Steel Research, Vol. 65,2009, pp1269-1278

- [13] ABAQUS theory manual, (2003) Version 6.7 Hibbitt, Karlsson and Sorensen, Inc. Pawtucket, R.I.
- [14] British Standards Institution. BS 5950: Structural use of steelwork in buildings, Part 1: Code of practice for design — rolled and welded sections, London (UK).
- [15] British Standards Institution. BS 8110, Structural use of concrete, Part 1: Code of practice for design and Construction, London (UK).
- [16] Wang Jing-Feng, Li Guo-Qiang. Testing of semi-rigid steelconcrete composite frames subjected to vertical loads. Engineering Structures 2007;29(8): 1903-16.
- [17] ATBLAST 2.0, Applied Research Associates,2000
- [18] US DEPARTMENTS OF THE ARMY, NAVY AND AIRFORCE, Technical Manual, Army TM5-1300, Navy NAVFAC P-397, Air Force AFR 88-22,Structures to resist the effects of accidental explosions, US Department of Commerce, National Technical Information Service, Washington, DC, 1990
- [19] HOPKINSON, B. British Ordnance board minutes 13565, 1915
- [20] CRANZ, C., Lehrbuch der Ballistik, Springer, Berlin, 1926

TABLE 1.1 SECTION PROPERTIES FROM BS5950

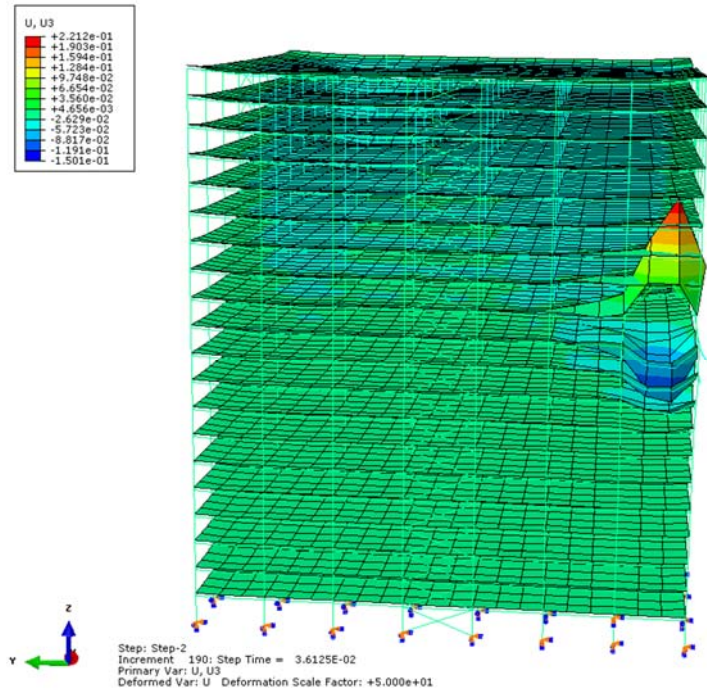
Section Designation	Mass per Meter Kg/m	Depth of Section D mm	Width of Section B mm	Web thickness mm	Flange thickness mm	Root Radius mm
UC356X406X634	633.9	474.6	424.0	47.6	77	15.2
UC356X406X467	467.0	436.6	412.2	35.8	58	15.2
UC356X406X287	287.1	393.6	399	22.6	36.5	15.2
UB533X210X92	92.1	533.1	209.3	10.1	15.6	12.7

TABLE 1.2 SECTION PROPERTIES FROM BS5950

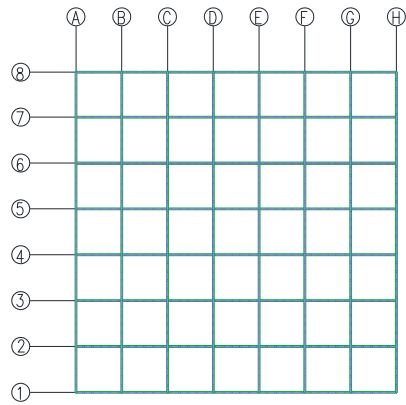
Section Designation	Mass per Meter Kg/m	Depth of Section D mm	thickness mm	Root Radius mm
CHCF 273X12.5	80.3	273	12.5	9.22

TABLE 2 RESULT COMPARISON OF TWO METHODS

	Method of this paper	Alternative path Method
Axial Force of Beam B1-A1 at level 13	884 kN	320kN
Shear Force of Beam B1-A1 at level 13	91 kN	7.9kN
Moment of Beam B1-A1 at level 13	100 kN.m	27kN.m
Compressive Force of Column B1 at level 12	1460 kN	1700 kN
Shear Force of Column B1 at level 12	220kN	35kN



a. Isotropic view (blast detonated at level 12, deformation is amplified)



b. Typical General Arrangement and Grid

Fig. 1 The analysis model

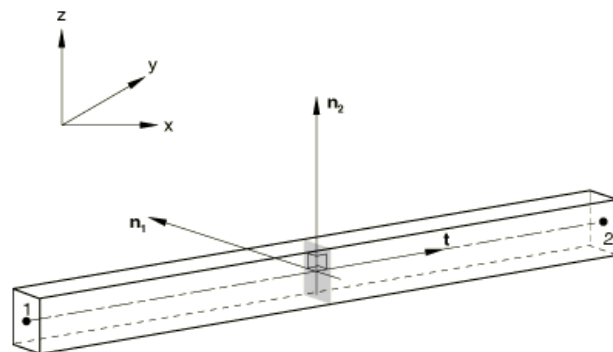


Fig. 2 Local axis definition for beam-type elements in ABAQUS [13]

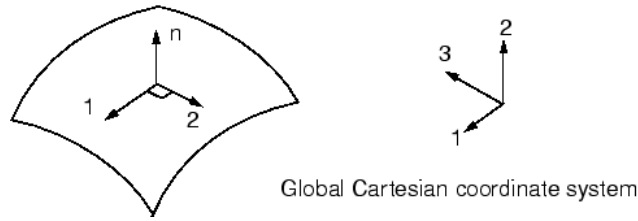


Fig. 3 Default local shell material directions in ABAQUS [13]

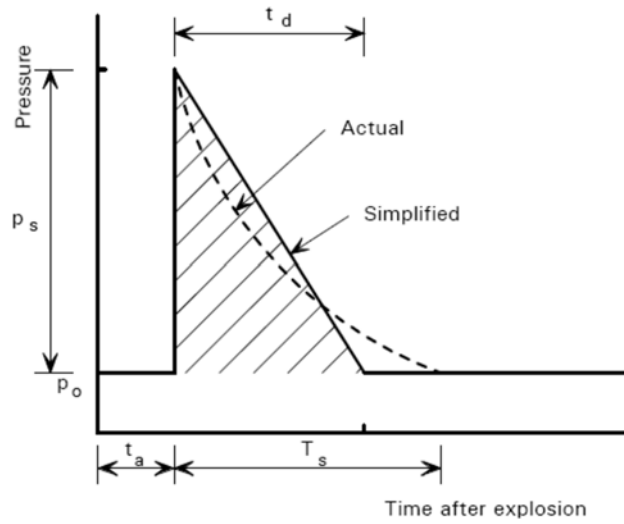


Fig.4 Simplified blast-wave overpressure profile with impulse by [3]

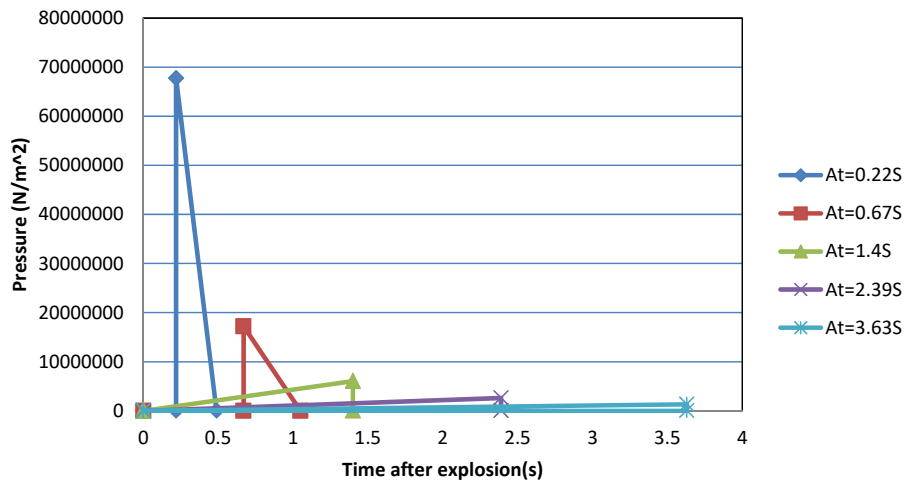
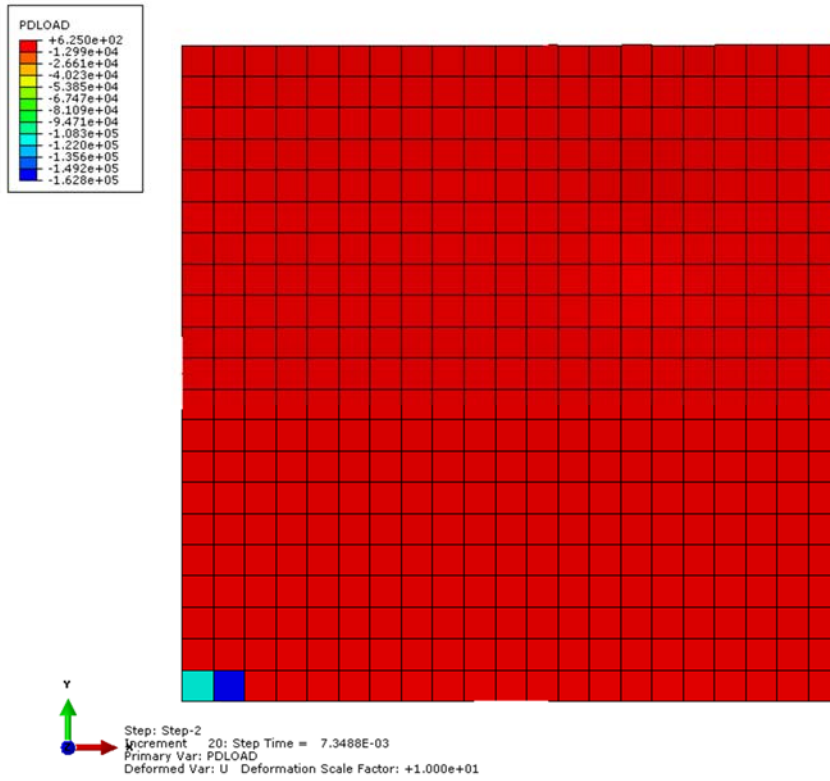
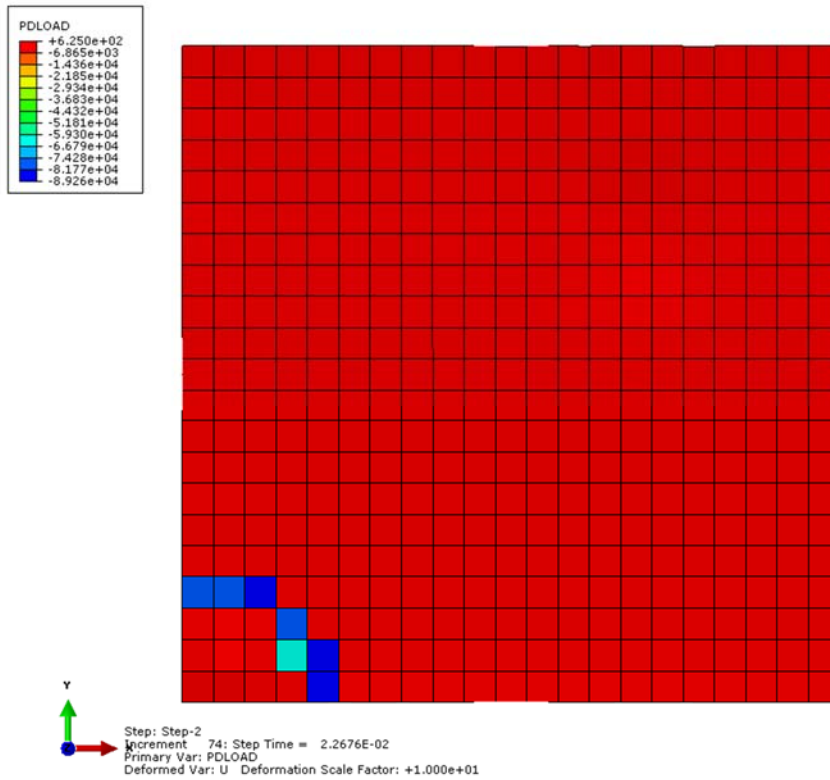


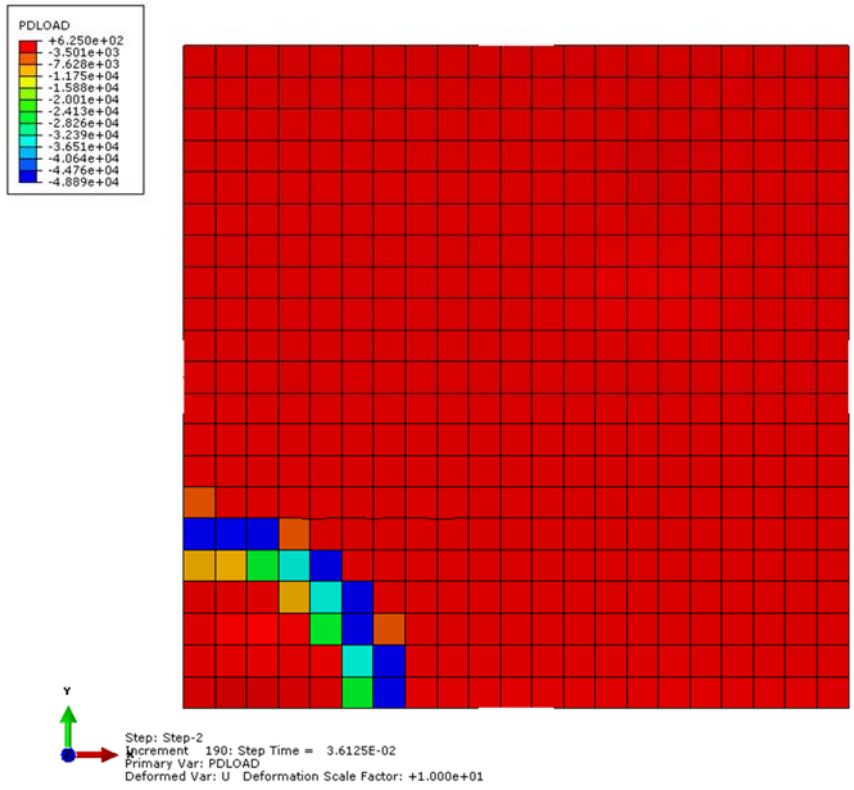
Fig.5 Blast overpressure profile at different Arrival time (At) of the proposed analysis model



a. Time=0.007(s)



b. Time=2.26e-2(s)



c. Time=3.61e-2(s)

Fig6. Distribution of blast load Pressure on the slabs on level 13 at different time

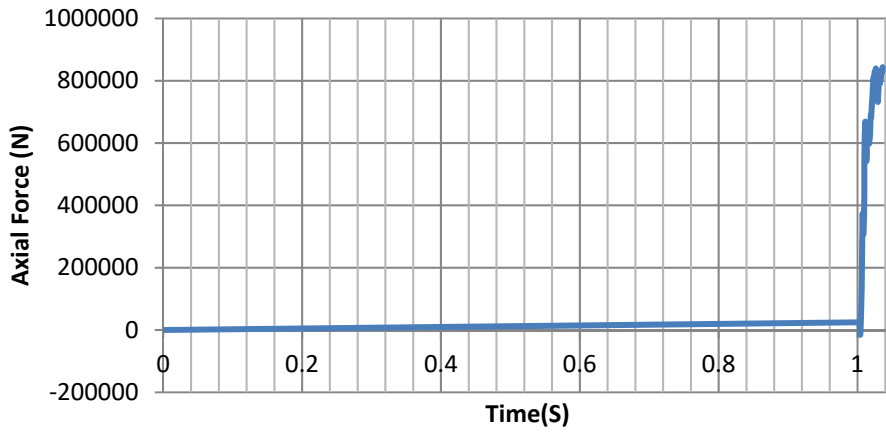


Fig 7. Axial force of beam B1-A1 at level 13

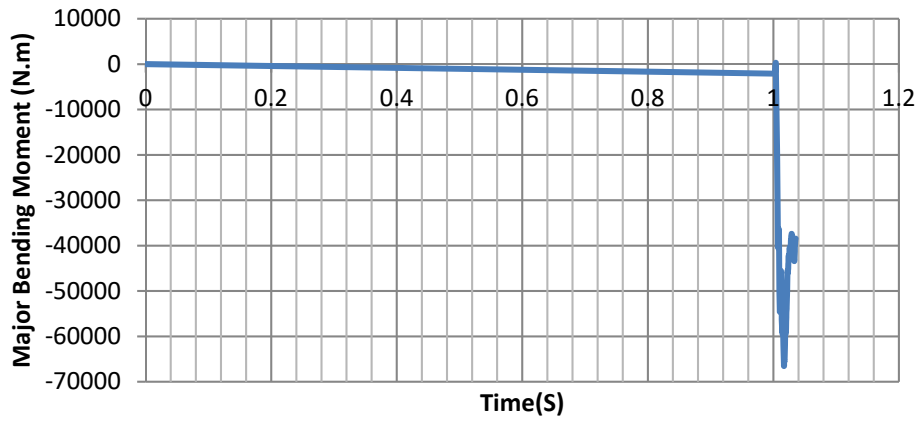


Fig 8. Major bending Moment of beam B1-A1 at level 13

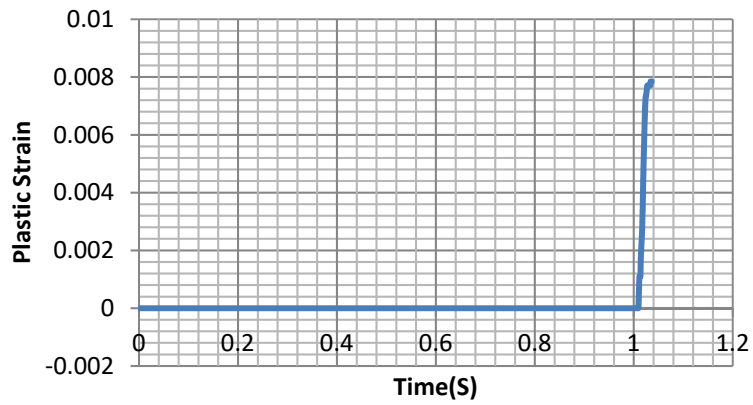


Fig.9 Plastic strain of beam B1-A1 at level 13

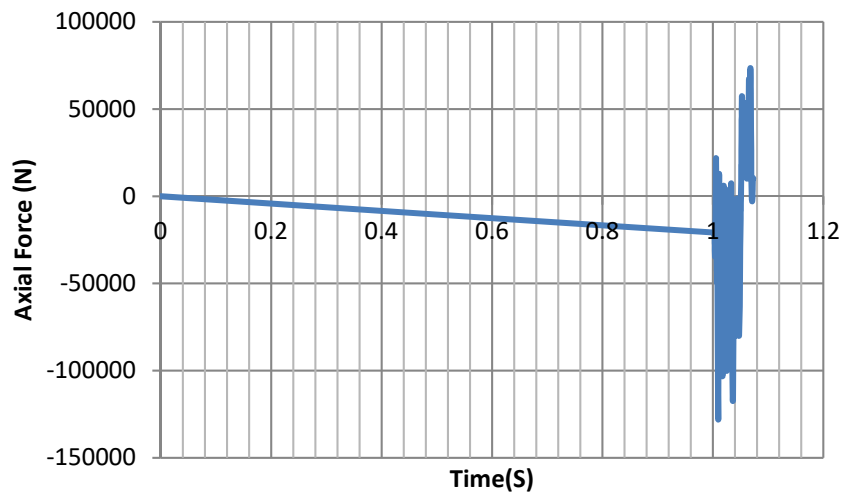


Fig.10 Axial force of beam D1-C1 at level 13

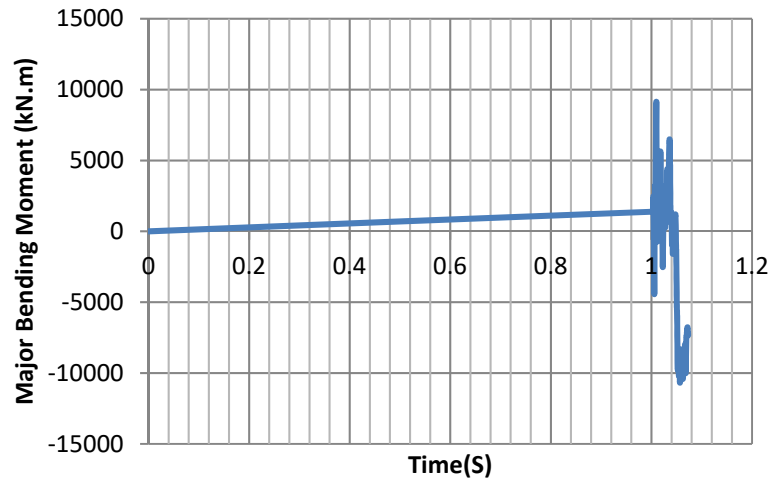


Fig.11 bending moment of beam D1-C1at level 13

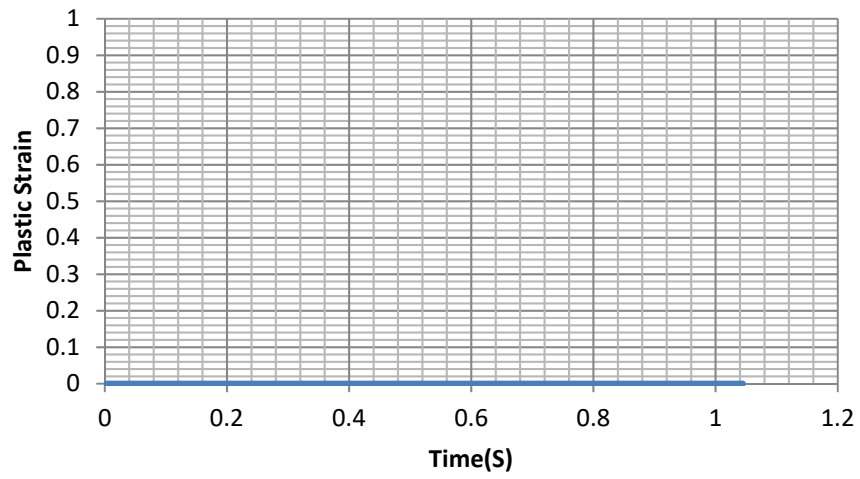


Fig.12 Plastic strain of beam D1-C1 at level 13

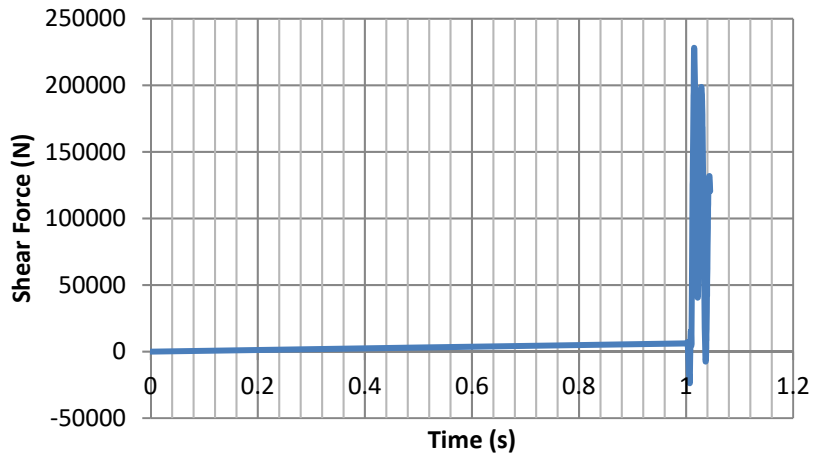


Fig 13. Shear force of column B1 at level12

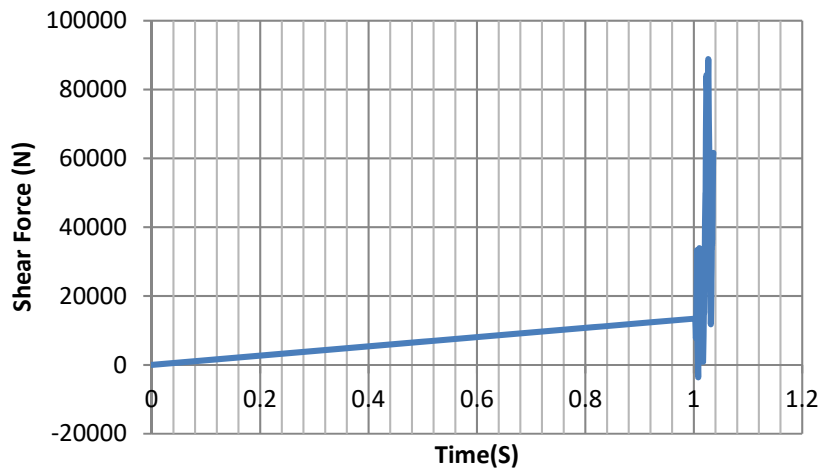


Fig 14. Shear force of column B2 at level12

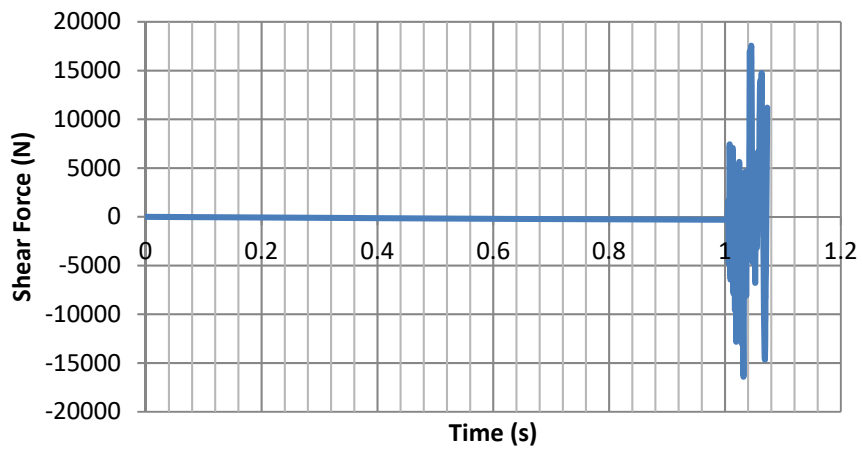


Fig.15 Shear force of column D4 at level12

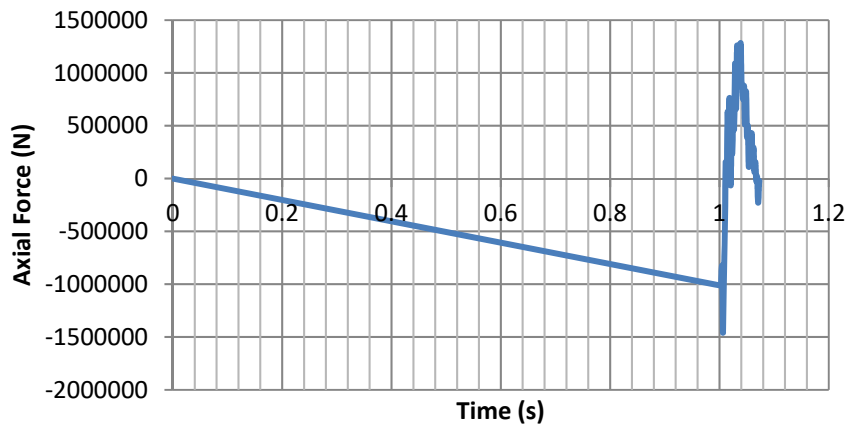


Fig. 16 Axial force of column B1 at level12

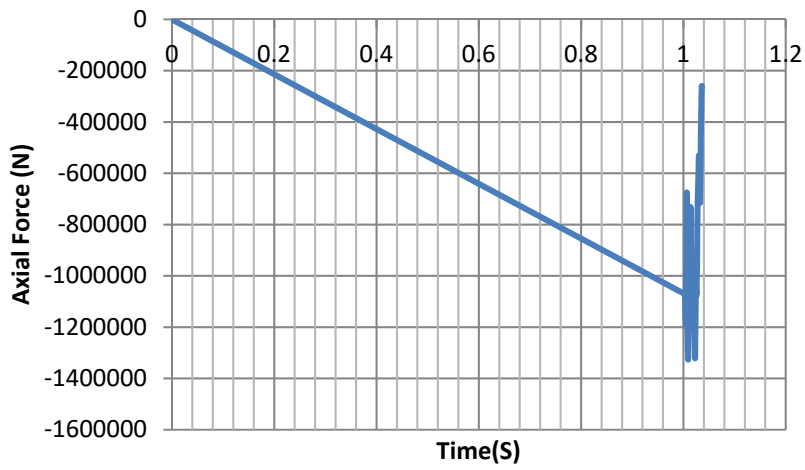


Fig.17 Axial force of column C1 at level 12

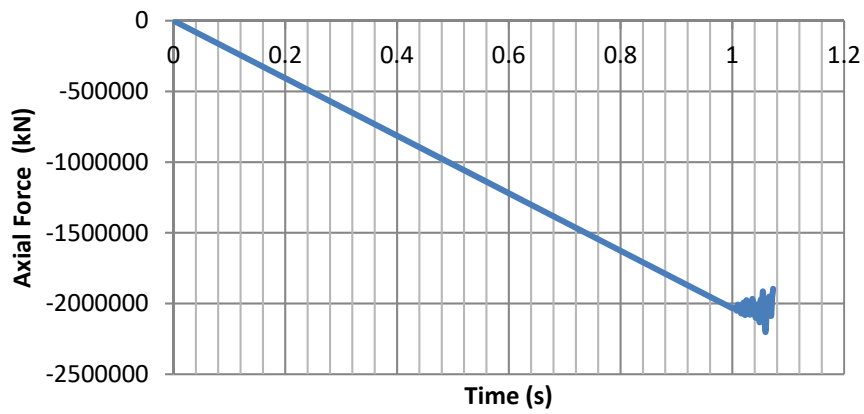


Fig.18 Axial force of column D4 at level 12

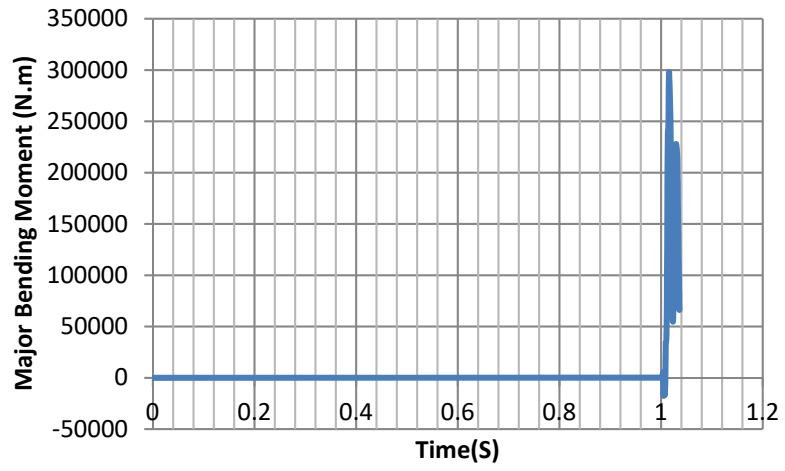


Fig. 19 Bending moment of column B1 at level12

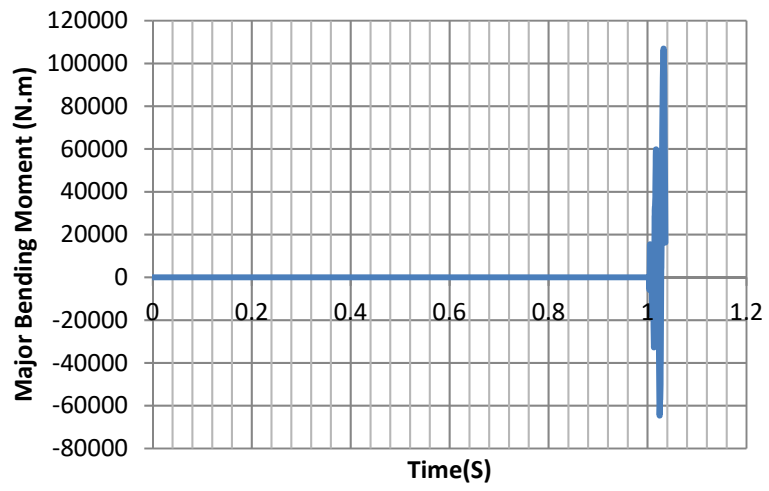


Fig. 20 Bending moment of column C1 at level12

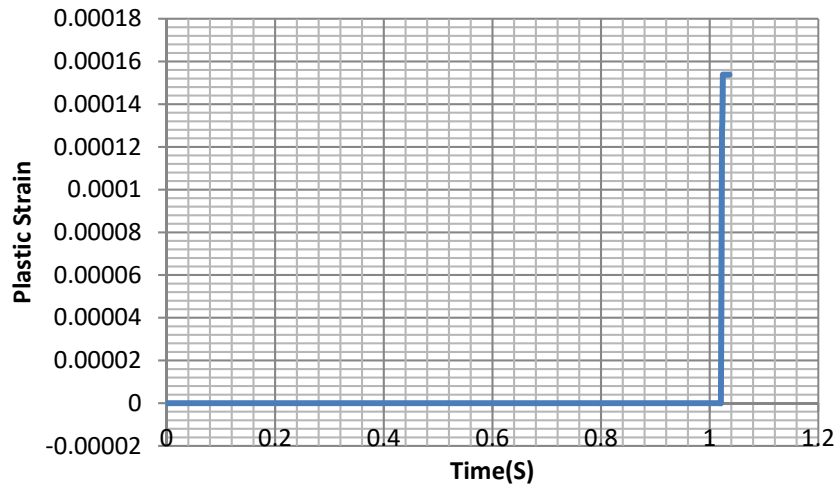


Fig. 21 Plastic strain of column A1 at level12

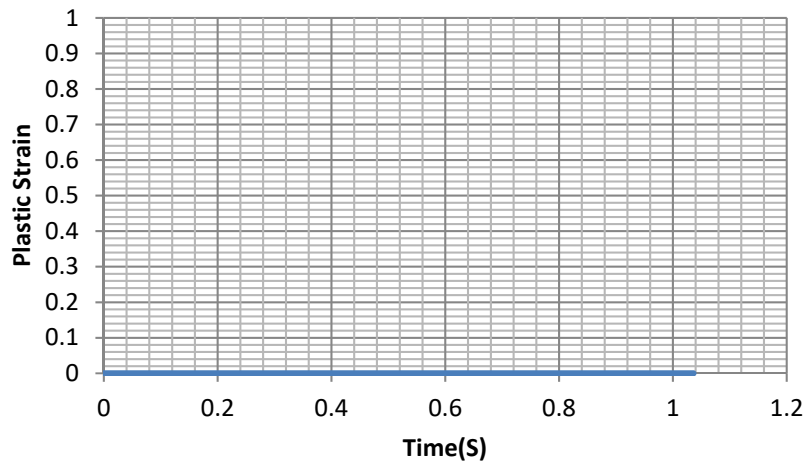


Fig. 22 Plastic strain of column C1 at level12

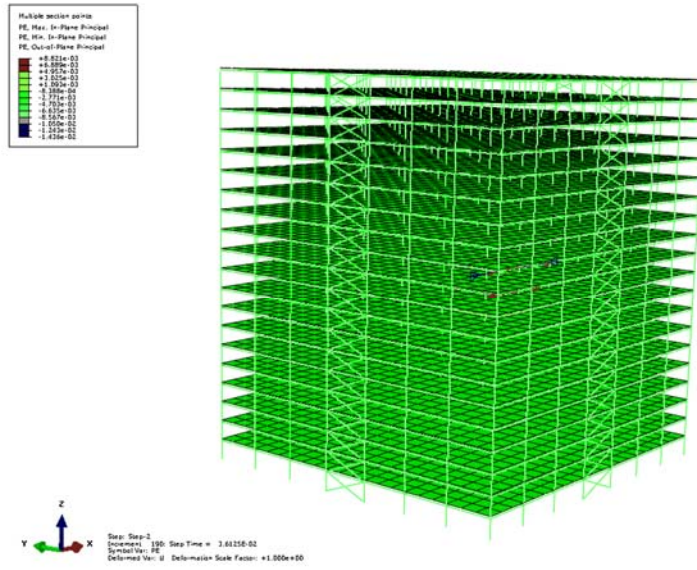


Fig.23 Concentrations of plastic strain in the composite slab depicting crack patterns

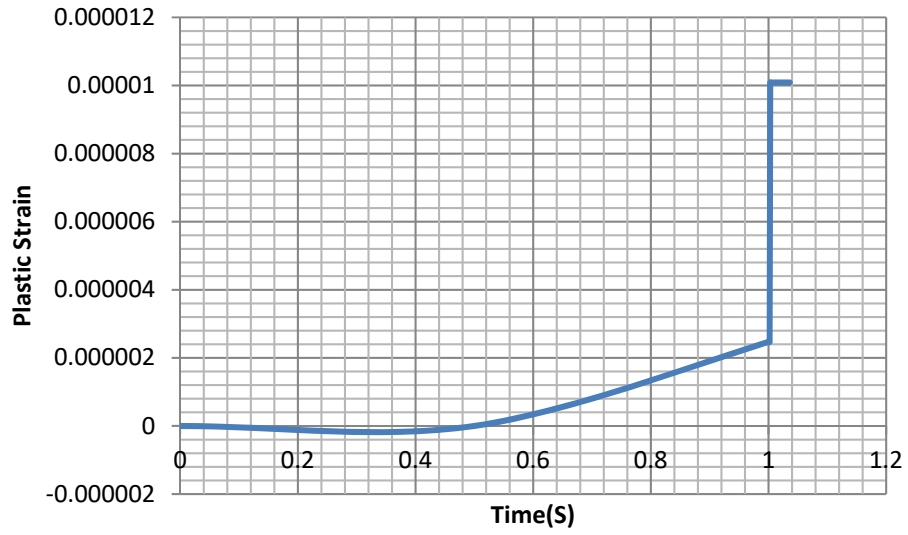


Fig. 24 Plastic strain of slab A1-B1-B2-A2 at level13